Nano Research
2019, 12(4): 855–861

ISSN 1998-0124 CN 11-5974/O4
https://doi.org/10.1007/s12274-019-2308-9

Research Article

Chemotherapy drugs derived nanoparticles encapsulating mRNA encoding tumor suppressor proteins to treat triple-negative breast cancer

Chengxiang Zhang[1,§], Xinfu Zhang[1,†,§], Weiyu Zhao[1,§], Chunxi Zeng[1], Wenqing Li[1], Bin Li[1], Xiao Luo[1], Junan Li[2], Justin Jiang[1], Binbin Deng[3], David W. McComb[3,4], and Yizhou Dong[1,5,6,7,8,9] (✉)

[1] *Division of Pharmaceutics & Pharmaceutical Chemistry, College of Pharmacy, The Ohio State University, Columbus, OH 43210, USA*
[2] *College of Pharmacy, The Ohio State University, Columbus, OH 43210, USA*
[3] *Center for Electron Microscopy and Analysis, The Ohio State University, Columbus, OH 43212, USA*
[4] *Department of Materials Science and Engineering, The Ohio State University, Columbus, OH 43210, USA*
[5] *Department of Biomedical Engineering, The Ohio State University, Columbus, OH 43210, USA*
[6] *The Center for Clinical and Translational Science, The Ohio State University, Columbus, OH 43210, USA*
[7] *The Comprehensive Cancer Center, The Ohio State University, Columbus, OH 43210, USA*
[8] *Dorothy M. Davis Heart & Lung Research Institute, The Ohio State University, Columbus, OH 43210, USA*
[9] *Department of Radiation Oncology, The Ohio State University, Columbus, OH 43210, USA*
[†] *Present address: State Key Laboratory of Fine Chemicals, Dalian University of Technology, Dalian 116024, China*
[§] *Chengxiang Zhang, Xinfu Zhang, and Weiyu Zhao contributed equally to this work.*

Received: 28 December 2018 / **Revised:** 17 January 2019 / **Accepted:** 20 January 2019

ABSTRACT

Triple-negative breast cancer (TNBC) is one type of the most aggressive breast cancers with poor prognosis. It is of great urgency to develop new therapeutics for treating TNBC. Based on current treatment guideline and genetic information of TNBC, a combinational therapy platform integrating chemotherapy drugs and mRNA encoding tumor suppressor proteins may become an efficacious strategy. In this study, we developed paclitaxel amino lipid (PAL) derived nanoparticles (NPs) to incorporate both chemotherapy drugs and P53 mRNA. The PAL P53 mRNA NPs showed superior properties compared to Abraxane® and Lipusu® used in the clinic including high paclitaxel loading capacity (24 wt.%, calculated by paclitaxel in PAL), PAL encapsulation efficiency (94.7% ± 6.8%) and mRNA encapsulation efficiency (88.7% ± 0.7%). Meanwhile, these NPs displayed synergetic cytotoxicity of paclitaxel and P53 mRNA in cultured TNBC cells. More importantly, we demonstrated *in vivo* anti-tumor efficacy of PAL P53 mRNA NPs in an orthotopic TNBC mouse model. Overall, these chemotherapy drugs derived mRNA NPs provide a new platform to integrate chemotherapy and personalized medicine using tumor genetic information, and therefore represent a promising approach for TNBC treatment.

KEYWORDS

paclitaxel amino lipid derived nanoparticles, mRNA therapeutics, combination therapy, triple-negative breast cancer

1 Introduction

Triple-negative breast cancer (TNBC) has been defined as a subtype of breast cancer with low expression of estrogen receptors (ER), progesterone receptors (PR), and human epidermal growth factor receptors (HER2) [1]. Because TNBC lacks the therapeutic targets mentioned above, these tumors progress aggressively and lead to poor treatment outcome for TNBC patients [2, 3]. Consequently, there is an urgent demand to develop effective therapeutics for treating TNBC. Previous studies reported that combinational therapy improved therapeutic efficacy in comparison to single medicine, which provided a potential treatment strategy for hard-to-treat cancers [4, 5], such as TNBC [6]. Currently, chemotherapy drugs are the main regimens in the systemic treatment guideline for TNBC [2]. Meanwhile, our understanding of tumorigenesis and relevant genetic information of TNBC establish the opportunity for personalized medicine [7]. According to previous tumor genetics studies on TNBC, mutation of tumor suppressor gene (TSG) TP53 was found in single most high rate (50%–80%) in TNBC patients' samples [8]. The wild type P53 protein suppresses aberrant cell cycles and assists apoptosis [9] while the mutant P53 protein fails to induce such responses [10]. Based on the characteristics of TNBC, we hypothesized that a combinational therapy combining chemotherapy drugs and personalized medicine based on genetic information may construct an effective platform for TNBC treatment.

To test this concept, we first synthesized chemotherapy drugs derived amino lipids (Fig. 1). Then, we formulated these lipids with P53 mRNA to afford a nanoparticle platform integrating both chemotherapy drugs and personalized medicine. This platform holds several favorable features. For example, chemotherapy drugs can be fine-tuned if TNBC is sensitive to a specific drug. Moreover, in the case that other tumor suppressor gene is identified for a TNBC patient population, the platform is capable of delivering mRNA encoding that particular TSG. Furthermore, mRNA transcripts introduce transient translation in the cytoplasm that avoids the risk of insertional mutagenesis in the genome [11–28]. Encouraged by

Address correspondence to dong.525@osu.edu

previous research findings in Ref. [17], we designed and prepared chemotherapy drugs derived lipid conjugates containing ionizable amino groups. In addition to their mRNA encapsulation ability, these drug–lipid conjugates can also potentially increase the apparent solubility of water-insoluble drugs [29] as well as drug loading capacity when formulated into nanoparticles [30]. Because chemotherapy drugs derived amino lipids have strong interactions with mRNA, these nanoparticles are able to simultaneously deliver these two types of therapeutics to the same tumor cells, resulting in optimal combinational effects.

Consistent with our design, we found the formulated paclitaxel amino lipid (PAL) P53 mRNA nanoparticles (NPs) exhibited high paclitaxel loading capacity (24 wt.%), which is higher than that of two clinically used paclitaxel formulations, Abraxane® (paclitaxel, ~ 10 wt.%) [31], an albumin bonded paclitaxel, and Lipusu® (paclitaxel, ~ 7 wt.%) [32], a liposomal paclitaxel nanoparticle. Other favorable characteristics included its high paclitaxel encapsulation efficiency (94.7% ± 6.8%) and high mRNA encapsulation efficiency (88.7% ± 0.7%). These PAL mRNA NPs were capable of loading different kinds of mRNAs and expressing functional protein in MDA-MB-231 cells, a human TNBC cell line. Moreover, the PAL P53 mRNA NPs showed significant anti-tumor efficacy in an orthotopic TNBC mouse model. This proof-of-concept study supports the rationale of a nanoparticles platform combining chemotherapy drugs and mRNAs encoding tumor suppressor proteins as a potential treatment for TNBC.

2 Results

2.1 Synthesis of chemotherapy drugs derived amino lipids

First, we selected two representative anti-breast cancer agents, paclitaxel and camptothecin [33, 34]. As shown in Fig. 1(a), we installed amino lipid on paclitaxel and camptothecin, respectively through an ester bond. These two compounds were named PAL and camptothecin amino lipid (CAL). PAL and CAL shared the same lipid chains which contained two tertiary amines that could be ionized at acidic pH environment and interact with mRNA molecules (Fig. S1 in the Electronic Supplementary Material (ESM)). The structures of PAL and CAL were confirmed by ^{1}H NMR and mass spectrum (MS).

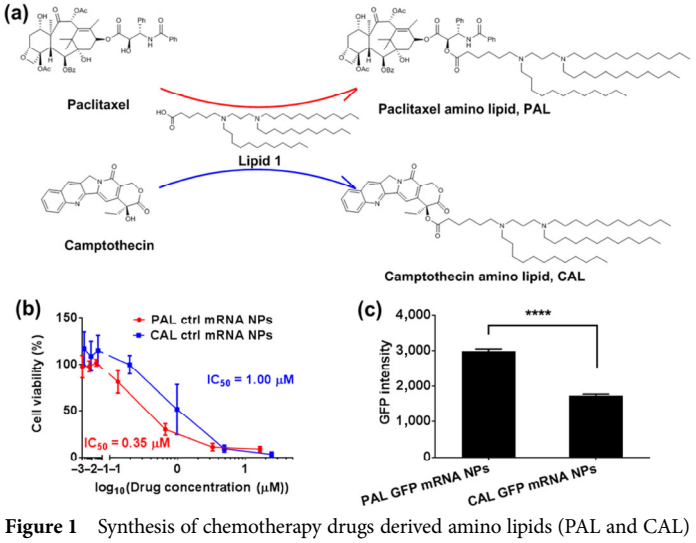

Figure 1 Synthesis of chemotherapy drugs derived amino lipids (PAL and CAL) and characterization of their formulated nanoparticles in MDA-MB-231 cells. (a) Synthetic routes to chemotherapy drugs derived amino lipids. Paclitaxel and camptothecin were conjugated with lipid 1 to afford PAL and CAL. (b) IC_{50} of PAL and CAL ctrl mRNA NPs were determined using an MTT assay. Data were presented as mean ± SD (n = 3). (c) GFP intensity was measured after delivery of PAL or CAL GFP mRNA NPs in MDA-MB-231 cells. Data were presented as mean ± SD (n = 3) (Student's t-test, ****, $p < 0.0001$).

2.2 Characterization of chemotherapy drugs derived mRNA nanoparticles

Next, we formulated either PAL or CAL with 1,2-dioleoylsn-glycero-3-phosphoethanolamine (DOPE), cholesterol (Chol), 1,2-dimyristoyl-rac-glycero-3-methylpolyoxyethylene (DMG-PEG_{2000}, PEG) (molar ratio: conjugate/DOPE/Chol/DMG-PEG_{2000} = 20/30/40/0.75), and a non-toxic control mRNA (ctrl mRNA) to prepare the nanoparticles as reported previously [35–37]. PAL and CAL mRNA NPs have similar particle properties including the size distribution and zeta potential (Fig. S2 in the ESM). In order to compare the cytotoxicity of these two NPs, we performed an 3-(4,5-dimethylthiazol-2-yl)-2,5-diphenyltetrazolium bromide (MTT) assay in MDA-MB-231 cells, a human TNBC cell line. As shown in Fig. 1(b), PAL ctrl mRNA NPs were more potent (IC_{50} = 0.35 μM) than CAL ctrl mRNA NPs (IC_{50} = 1.00 μM). In addition, we studied the mRNA delivery efficiency of PAL and CAL mRNA NPs using GFP mRNA. To minimize the effects of cytotoxicity in affecting the results of flow cytometry, we treated MDA-MB-231 cells only 6 h and then green fluorescent protein (GFP) signals were measured by a flow cytometer. The results showed PAL GFP mRNA NPs also induced a significantly higher GFP signal compared with that in CAL GFP mRNA NPs (Fig. 1(c)). Thus, we chose PAL mRNA NPs for further formulation optimization.

2.3 Formulation optimization of chemotherapy drugs derived mRNA nanoparticles

We further optimized the PAL mRNA NPs by using an experimental orthogonal design to study the effects of each formulation components on mRNA delivery efficiency, including PAL, DOPE, Chol, and DMG-PEG_{2000} (Fig. 2(a)) [35]. An $L_{16}(4^4)$ orthogonal array was generated, and 16 different formulations were prepared and characterized according to this array (Table S1 and Figs. S3(a)–S3(c) in the ESM). The fluorescence-activated cell sorting (FACS) analysis (Fig. S3(d) in the ESM and Figs. 2(b)–2(e)) predicted the following molar ratio is the optimum: PAL/DOPE/Chol/DMG-PEG_{2000} = 30/50/40/0.15. However, because precipitation was found in the formulations with low level of DMG-PEG_{2000} (Table S1 in the ESM), we increased the PEG molar ratio and adjusted the formulation to PAL/DOPE/Chol/DMG-PEG_{2000} = 30/50/40/0.75 (formulation 17). The GFP signal of optimized formulation 17 was comparable to formulation 16, the highest one in the orthogonal array (Fig. S4 in the ESM). Thus, formulation 17 was used for the following studies.

Then, we prepared the nanoparticles using P53 mRNA with a FLAG tag sequence (Fig. S5(a) in the ESM) and evaluated its delivery *in vitro*. The optimized PAL P53 mRNA NPs formulation showed a relatively homogeneous peak in size distribution (Fig. 2(f)). PAL P53 mRNA NPs were in spherical morphology from the cryogenic electron microscopy (cryo-EM) image (Fig. 2(g)). After treatment of cells with PAL P53 mRNA NPs, we stained the cells via antibody against the FLAG tag. The green signal in Fig. 2(h) indicated apparent expression of P53 protein in these cells. We prepared PAL P53 mRNA NPs from different batches and observed similar fluorescence signal after P53 mRNA NPs treatment, demonstrating the reproducibility of these nanoparticles (Fig. S5(b) in the ESM). Particle size was 163.2 ± 0.9 nm with polydispersity index (PDI) of 0.10 ± 0.01 (day 0, Fig. S5(d) in the ESM). The stability test showed the FLAG signal were consistent after treatment with PAL P53 mRNA NPs stored at 4 °C for at least one week, which indicated that these nanoparticles were stable under the storage condition (Fig. S5(c) in the ESM). Similar results were noticed for particle size and its distribution (Fig. S5(d) in the ESM).

2.4 *In vitro* cytotoxicity of chemotherapy drugs derived mRNA nanoparticles

Before we tested the cytotoxic effect of PAL P53 mRNA NPs, we studied the TP53 mutation status of these MDA-MB-231 cells. The

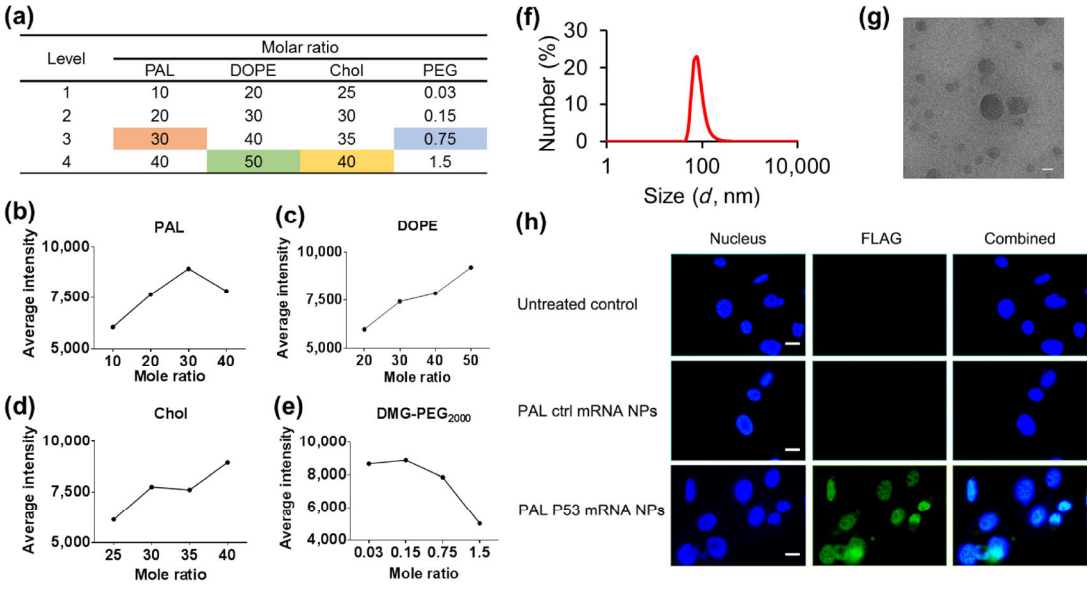

Figure 2 Formulation optimization of PAL mRNA NPs. (a) Four levels of each mRNA NPs' components. Highlighted numbers are the molar ratio of the four components in the optimized formulation. (b) PAL, (c) DOPE, (d) Chol, and (e) DMG-PEG$_{2000}$ (PEG) are the impact trend of each formulation component on GFP mRNA delivery. (f) Size distribution of the optimized PAL P53 mRNA NPs formulation. (g) Cryo-EM image of the optimized PAL P53 mRNA NPs formulation. Scale bar = 50 nm. (h) Imaging of FLAG tagged P53 protein *in vitro*. The FLAG tag was stained by anti-FLAG primary antibody and FITC-labeled secondary antibody 6 h after incubation with P53 mRNA NPs. Nucleus was stained by Hoechst 33342. Scale bar = 20 μm.

results showed a single nucleotide mutation from G to A (Fig. S6 in the ESM), which caused the corresponding amino acid change from arginine to lysine (R280K). This genetic mutation is same as that in Ref. [38]. Then, cytotoxicity of PAL P53 mRNA NPs were examined by the MTT assay in these cells. To study the combinatorial effects of paclitaxel (PTX) and P53 mRNA, we synthesized a control lipid without drug conjugate, amino lipid (AL, Fig. S1(a) in the ESM). Also, we included a non-toxic mRNA as a control for P53 mRNA (ctrl mRNA). Then, we formulated these four types of nanoparticles: AL ctrl mRNA NPs (PTX–, P53–), AL P53 mRNA NPs (PTX–, P53+), PAL ctrl mRNA NPs (PTX+, P53–) and PAL P53 mRNA NPs (PTX+, P53+). All these NPs shared similar characteristics (Figs. S7(a) and S7(b) in the ESM). As shown in Fig. 3(a), the cytotoxicity was in a dose-dependent manner. AL ctrl mRNA NPs showed minimum toxicity, while AL P53 mRNA NPs increased cytotoxicity at high doses of P53. Although both PAL ctrl mRNA NPs and PAL P53 mRNA NPs displayed dramatic inhibition of tumor cell growth, PAL P53 mRNA NPs were more active than PAL ctrl mRNA NPs ($p < 0.001$ at an mRNA dose of 63 ng per well and $p < 0.05$ at an mRNA dose of 125 ng per well). We also calculated the combination index (CI = 0.937 < 1) from the data of PAL ctrl mRNA NPs (PTX+, P53–), AL P53 mRNA NPs (PTX–, P53+), and PAL P53 mRNA NPs (PTX+, P53+), which indicated a synergetic effect between paclitaxel and P53 mRNA. Meanwhile, we measured the PTX encapsulation efficiency and release profile of PAL P53 mRNA NPs. Quantitative results gave a 94.7% ± 6.8% of PTX encapsulation efficiency in the PAL P53 mRNA NPs (Fig. S7(c) in the ESM). At the 48- and 72-hour time points, around 37% and 84%, respectively of PAL was released (Fig. 3(b)).

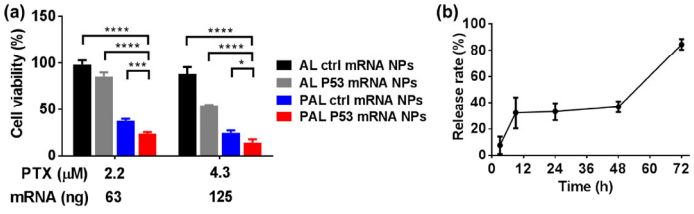

Figure 3 *In vitro* cytotoxicity of PAL P53 mRNA NPs. (a) Cytotoxicity of PAL P53 mRNA NPs was determined by the MTT assay. Data were presented as mean ± SD ($n = 3$) (Student's *t*-test, ****, $p < 0.0001$, ***, $p < 0.001$, *, $p = 0.015$). (b) PAL release profile of PAL P53 mRNA NPs. Data were presented as mean ± SD ($n = 3$).

2.5 *In vivo* anti-tumor efficacy of chemotherapy drugs derived mRNA nanoparticles

Given the encouraging *in vitro* results of PAL P53 mRNA NPs, we established an orthotopic TNBC model in nude mice to test its *in vivo* anti-tumor activity. Five groups ($n = 8$) were included: phosphate buffered saline (PBS) control group (PBS), free P53 mRNA group (P53 mRNA), free PTX treatment group (PTX), PAL ctrl mRNA NPs treatment group (PAL ctrl mRNA NPs), and PAL P53 mRNA NPs treatment group (PAL P53 mRNA NPs). Tumor size was measured every day after the first treatment. Since several mice in the PBS group (4 mice) and free P53 mRNA group (3 mice) reached the end points at the day 13 after treatment, Fig. 4(a) was plotted till day 12 with at least 7 mice in each group.

PAL P53 mRNA NPs showed significantly stronger inhibition of tumor growth in comparison to other groups (Fig. 4(a)). Specifically, one mouse in PAL P53 mRNA NPs group (mouse 779) showed complete tumor elimination after treatments, which was confirmed by observation, touching and *in vivo* imaging of luciferase signal (Fig. S8 in the ESM). More importantly, the Kaplan-Meier survival curves showed PAL P53 mRNA NPs treatment significantly extended the median survival time of tumor bearing mice compared to other four groups (Fig. 4(b)). PAL ctrl mRNA NPs and PTX free drug treatment groups exhibited tumor inhibition to some extent, and their efficacy was much weaker than that of PAL P53 mRNA NPs treatment group. Obvious FLAG signal in the dissected tumor tissue was noticed in consistent with the *in vitro* imaging, suggesting the expression of P53 proteins in tumors (Fig. 4(c)). The body weight of mice from all five groups were comparable (Fig. S9 in the ESM).

3 Conclusion

In summary, we aim to test the hypothesis that a combination of chemotherapy drugs and personalized medicine may offer a superior strategy for treating TNBC. On one hand, chemotherapy drugs are widely used small molecule anti-tumor agents for TNBC. On the other hand, personalized medicine is based on the analysis of genetic

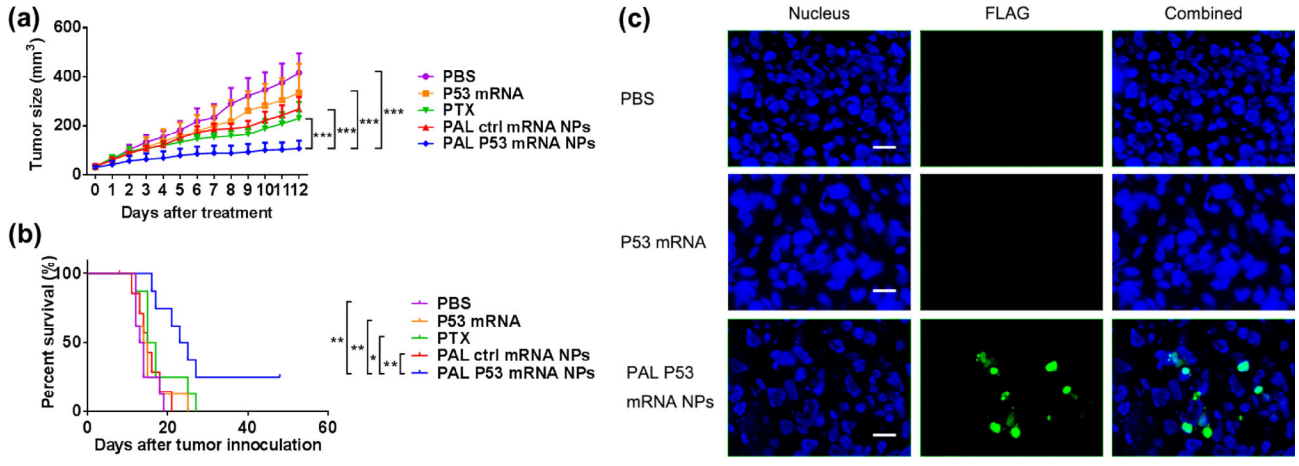

Figure 4 *In vivo* anti-tumor activity of PAL P53 mRNA NPs. (a) Tumor size. Inhibition of tumor growth by i.v. injection of PAL P53 mRNA NPs was significantly stronger than other groups. Data were presented as mean ± SD (n = 7 or 8) (two-way ANOVA with repeated measurements, ***, $p < 0.001$). (b) Overall survival of tumor bearing mice. Intravenous PAL P53 mRNA NPs treatment significantly extended the median survival time of tumor bearing mice (log-rank test, **, $p < 0.01$, *, $p = 0.041$). (c) P53 protein was observed in tumor tissues from PAL P53 mRNA NPs treated mice, while not from PBS or P53 mRNA treated mice. Scale bar = 50 μm.

information from TNBC patients [8]. For example, a large percentage of TNBC patients possesses P53 loss or mutation. To prove this concept, we designed and developed a PAL P53 mRNA nanoparticles (PAL P53 mRNA NPs). PTX was used as a chemotherapy drug in the current TNBC treatment guideline [2]. PTX has low water solubility and the most widely used formulation Taxol® uses Cremophor EL® and ethanol to increase the solubility of PTX in water [31]. However, the formulation vehicle Cremophor EL® was known to cause unfavorable hypersensitivity, which required the patients to take premedication [39]. We formulated the paclitaxel in the newly synthesized PAL with other formulation components: DOPE, Chol, and DMG-PEG$_{2000}$ to encapsulate mRNA molecules and prepare PAL P53 mRNA NPs. The formulation composition was optimized by an orthogonal array to maximize its mRNA delivery efficiency. The optimized formulation was stable for at least one week under 4 °C. Moreover, the high PTX loading capacity (24 wt.%), PTX encapsulation efficiency (94.7% ± 6.8%) and extended drug release profile were favorable for *in vivo* applications. When we incorporated P53 mRNA in the optimized formulation and treated it with MDA-MB-231 cells, PAL P53 mRNA NPs showed synergetic cytotoxicity from its two types of therapeutic components: PTX and P53 mRNA. In addition to the promising *in vitro* anti-tumor activity, PAL P53 mRNA NPs (equivalent to 10 mg/kg PTX, 2 mg/kg P53 mRNA) induced strong therapeutic efficacy by inhibiting tumor growth and extending the overall survival of tumor bearing mice. In conclusion, this proof-of-concept study demonstrated that this nanoparticle platform combining chemotherapy drugs and tumor genetic information merit further development for TNBC therapy. Such a nanomaterial platform is applicable to the broad category of chemotherapy drugs and tumor suppressor genes for treating other types of cancers.

4 Materials and methods

4.1 Materials

All chemicals were purchased from Sigma-Aldrich (St. Louis, MO, USA) unless otherwise specified. Paclitaxel and camptothecin were purchased from Medkoo Biosciences (Morrisville, NC, USA). DOPE was purchased from Avanti Polar Lipids, Inc (Alabaster, AL, USA). DMG-PEG$_{2000}$ was purchased from NOF America Corporation (White Plains, NY, USA). The human MDA-MB-231-luc (MDA-MB-231) cells were the kind gift from Dr. Peixuan Guo's lab, and were cultured in DMEM/F12 culture medium containing 10% fetal bovine serum (FBS). MTT was purchased from Amresco (Solon, OH, USA). Anti-FLAG primary antibody (ab-1162) and fluorescein isothiocyanate (FITC) labeled secondary antibody (ab-6717) were purchased from Abcam (Cambridge, MA, USA). DNA extraction (DNeasy®) and purification (QIAquick®) kits were purchased from QIAGEN (Germantown, MD, USA). P53 primers were ordered from Eurofins Genomics, LLC (Louisville, KY, USA). Animal experiments were approved by the Ohio State University Institutional Animal Care and Use Committee (IACUC).

4.2 Synthesis of control lipids and chemotherapy drugs derived amino lipids

4.2.1 *Synthesis of AL*

Compounds b and c were synthesized according to methods reported previously [35, 40]. A solution of compound c (500 mg, 1.58 mmol) in CH_2Cl_2 (2 mL) was added excess amount of trifluoroacetic acid (2 mL). The mixture was stirred at room temperature (RT) for 2 h and monitored with thin layer chromatography. Upon completion of the reaction, the solvent was evaporated to yield oil like intermediate. The intermediate was dissolved in 20 mL of anhydrous tetrahydrofuran, followed by adding triethylamine (0.5 mL). The resulting mixture was stirred for 30 min at RT. After adding dodecyl aldehyde (1.5 g, 7.9 mmol) and $NaBH(OAc)_3$ (1.7 g, 7.9 mmol), the reaction mixture was stirred at RT for 24 h. After the solvent was removed, the residue was purified by column chromatography using a CombiFlash Rf system with a RediSep Gold Resolution silica column (Teledyne Isco) with gradient elution (CH_2Cl_2 and ultra) from 100% CH_2Cl_2 to 70% CH_2Cl_2 (ultra, CH_2Cl_2/MeOH/NH_4OH = 75/22/3 by volume) to give 400 mg AL, yield 35%. ^{1}H NMR (400 MHz, $CDCl_3$) δ = 4.17–4.11 (2H, m), 2.70–2.57 (11H, m), 2.33–2.29 (2H, t, J = 8), 1.78 (2H, s), 1.69–1.62 (3H, m), 1.54–1.48 (8H, m), 1.28 (59H, s), 0.92–0.88 (9H, t, J = 8). MS (m/z): $[M+H]^+$ calcd. for $C_{47}H_{97}N_2O_2$, 721.7542; found, 721.7526.

4.2.2 *Synthesis of PAL*

AL (250 mg, 0.35 mmol) was dissolved in 1.5 mL tetrahydrofuran (THF) and 1.5 mL MeOH, followed by adding 1.5 mL NaOH aqueous (1 M). The reaction mixture was stirred at 70 °C for 3 h. After adding 100 mL CH_2Cl_2, the mixture was dried with $MgSO_4$. After the solvent was removed, the residue was dissolved in 10 mL anhydrous CH_2Cl_2. To the solution was added paclitaxel (296 mg, 0.35 mmol), 1-ethyl-3-(3-dimethylaminopropyl) carbodiimide (EDC) (80 mg, 0.42 mmole) and N,N′-dimethyl-1,3-propanediamine (DMPA) (10 mg, 0.08 mmol). The resulting mixture was stirred at RT overnight.

After the solvent was removed, the residue was purified by column chromatography using a CombiFlash Rf system with a RediSep Gold Resolution silica column (Teledyne Isco) with gradient elution (CH_2Cl_2 and ultra) from 100% CH_2Cl_2 to 75% CH_2Cl_2 (ultra, CH_2Cl_2/MeOH/NH_4OH = 75/22/3 by volume) to give 275 mg PAL, yield 52%. ^{1}H NMR (400 MHz, $CDCl_3$): δ = 8.17–8.15 (2H, d, J = 8), 7.77–7.75 (2H, d, J = 8), 7.63–7.61 (1H, m), 7.56–7.51 (3H, m), 7.45–7.36 (6H, m), 6.32–6.29 (2H, d, J = 12), 6.00–5.97 (2H, m), 5.71–5.70 (1H, d, J = 4), 5.54–5.53 (1H, d, J = 4), 5.01–4.98 (1H, d, J = 12), 4.35 (1H, m), 4.33 (1H, m), 4.24–4.22 (1H, m), 3.85–3.83 (1H, d, J = 8), 2.48 (3H, m), 2.44–2.35 (14H, m), 2.25 (3H, s), 1.97 (3H, s), 1.76 (1H, s), 1.71 (3H, s), 1.64–1.58 (5H, m), 1.43–1.42 (10H, m), 1.28 (57H, s), 1.16 (3H, s), 0.92–0.88 (9H, t, J = 8). MS (m/z): $[M+H]^+$ calcd. for $C_{92}H_{142}N_3O_{15}$, 1,529.0433; found, 1,529.0320.

4.2.3 *Synthesis of CAL*

AL (250 mg, 0.35 mmol) was dissolved in 1.5 mL THF and 1.5 mL MeOH, followed by adding 1.5 mL NaOH aqueous (1 M). The reaction mixture was stirred at 70 °C for 3 h. After adding 100 mL CH_2Cl_2, the mixture was dried with $MgSO_4$. After the solvent was removed, the residue was dissolved in 10 mL dry CH_2Cl_2. To the solution was added paclitaxel (121 mg, 0.35 mmol), EDC (80 mg, 0.42 mmol) and DMPA (10 mg, 0.08 mmol). The resulting mixture was stirred at RT overnight. After the solvent was removed, the residue was purified by column chromatography using a CombiFlash Rf system with a RediSep Gold Resolution silica column (Teledyne Isco) with gradient elution (CH_2Cl_2 and ultra) from 100% CH_2Cl_2 to 75% CH_2Cl_2 (ultra, CH_2Cl_2/MeOH/NH_4OH = 75/22/3 by volume) to give 50 mg CAL, yield 14%. ^{1}H NMR (400 MHz, $CDCl_3$): δ = 8.42 (1H, s), 8.26 (1H, m), 8.12 (1H, m), 7.97 (1H, m), 7.86 (1H, m), 7.71 (3H, m), 7.51–7.49 (1H, m), 7.29 (1H, m), 7.25–7.16 (1H, m), 5.72–5.68 (1H, d, J = 16), 5.46–5.41 (1H, d, J = 20), 5.31–5.28 (1H, m), 4.01 (1H, s), 2.52–2.40 (12H, m), 2.19 (1H, m), 1.67 (2H, s), 1.57 (2H, m), 1.44–1.28 (55H, m), 1.00 (3H, s), 0.90 (9H, s). MS (m/z): $[M+H]^+$ calcd. for $C_{65}H_{106}N_4O_5$, 1,023.8233; found, 1,023.8195.

4.3 Characterization of P53 mutation status in MDA-MB-231 cells

To check the P53 mutation status of our MDA-MB-231 cells, genomic DNA was extracted from cells using a DNA extraction kit (DNeasy®, QIAGEN, MD, USA). Polymerase chain reaction (PCR) was applied to amplify a 596bp length of genomic DNA across the reported mutation position within the P53 region in MDA-MB-231 cells. The forward primer used was 5'-GGGACCTCTTAACCTGTGGC-3', and the reverse primer was 5'-TCTTTGAGGCATCACTGCCC-3'. After purification, the sequence was determined by Sanger sequencing.

4.4 Preparation of P53 mRNA

The cDNA sequence encoding wild-type P53 of 393 amino acids was obtained from Ensembl (transcript ID: ENST00000269305.8). A fragment sequence coding a FLAG tag (GACTACAAGGACG ACGATGACAAG) and GS linker (ggatcc) was added to the 5' of P53 coding sequence [41]. The corresponding linear dsDNA template was ordered from IDT as a gBlock gene fragment and subsequently inserted into a pUC19 derived vector via Golden Gate assembly. The resulting plasmid was amplified by PCR to generate the DNA template for transcription. The uncapped mRNA encoding P53 was synthesized *in vitro* using AmpliScribe T7-Flash Transcription Kit (Lucigen) and purified with RNA Clean & Concentrator-25 (Zymo), following manufacturers' instructions. Cap-1 structure was added using the Vaccinia Capping System and Cap 2′-O-Methyltransferase (NEB). After determination of concentration by Nanodrop (Thermo), the mRNA was stored in 1×TE at −80 °C until use.

The length of the final P53 mRNA product was examined by running precast 0.8% agarose E-gel electrophoresis (Invitrogen). P53 mRNA was mixed with equal volume of denaturing loading buffer (8.1 M urea, 0.9 mM EDTA, 0.1% (m/v) xylene cyanol FF, 0.1% (m/v) bromophenol blue in 1×TBE) and ssRNA ladder (NEB) with 4× volume of RNA loading dye (NEB). Both P53 mRNA and ssRNA ladder were incubated at 90 °C for 90 s right before gel loading. After electrophoresis, image was taken in ChemDoc MP imaging system (Bio-Rad).

4.5 Preparation, optimization and characterization of mRNA NPs

The mRNA nanoparticles used *in vitro* were prepared by the pipetting method [35–37, 42]. The mRNA nanoparticles used *in vivo* were prepared using microfluidic device (Precision NanoSystems, Vancouver, BC, Canada). For both methods, the lipid compounds were dissolved in ethanol to the desired concentration, and mRNA was diluted in the citrate buffer (pH = 3). After well pipetting and mixing with the lipid compounds and mRNA solution, the mRNA nanoparticles were prepared. For *in vivo* use, we dialyze the freshly formulated mRNA nanoparticles in the PBS solution before intravenous (i.v.) injection. The size distribution and zeta potential of mRNA nanoparticles in water were determined by Zetasizer (Malvern, Westborough, MA, USA). mRNA encapsulation efficiency (EE%) was determined by RiboGreen assay [35].

To optimize the formulation, an $L_{16}(4^4)$ orthogonal array was generated (Table S1 in the ESM). 16 formulations were first prepared according to the orthogonal array, and their size, PDI and zeta potential were measured. Next, these formulations each encapsulating 100 ng GFP mRNA was added to MDA-MB-231 cells in a 24 wells plate for 6 h. The GFP intensity was then analyzed by a flow cytometer (LSR II, BD) and used to analyze the effects of formulation components.

PTX loading capacity was calculated by the following equation: PTX loading capacity % = (weight of equivalent PTX in formulated PAL P53 mRNA NPs)/(weight of all lipid materials (PAL + DOPE + Chol + DMG-PEG_{2000}) in formulated PAL P53 mRNA NPs) × 100%. PTX EE% was determined by mass spectrum quantification of PAL. PTX EE% = (amount of PAL after dialysis)/(amount of total PAL added) × 100%. Chloroform was added to breakdown and extract PAL from PAL P53 mRNA NPs. The organic phase was then separated with water phase by centrifuge at 14,000 g for 15 min. Next, the chloroform phase was transferred and mixed with methanol (chloroform:methanol=1:9, v/v) for MS quantification. The standard curve was established for quantification of PAL in paclitaxel encapsulation efficiency test (Fig. S7(c) in the ESM). Cryo-EM image was obtained using the same method as reported before [35]. Briefly, CryoTEM samples were prepared by applying a small aliquot (3 μL) of PAL P53 mRNA NPs to a specimen grid. After blotting away excess liquid, the grid was immediately plunged into liquid ethane to rapidly form a thin film of amorphous ice using Vitrobot Mark IV system (Thermo Fisher Scientific, Hillsboro). CryoTEM images were collected at a nominal magnification of 57,000× with Falcon direct electron detector on Thermo Scientific™ Glacios™ CryoTEM. The microscope was operated at an acceleration voltage of 200 kV. PTX release was determined by mass spectrum quantification of remaining PAL in the release solution at different time points. The release solution contained 0.5 mg/mL esterase in 0.1% Tween 20 PBS. After incubating mRNA nanoparticles in release solution for 3, 9, 24, 48, 72 h at 37 °C, 200 rpm, chloroform was added to breakdown and extract remaining PAL. The organic phase was then separated and tested following the same method used in paclitaxel encapsulation efficiency test.

4.6 *In vitro* delivery of P53 mRNA NPs in MDA-MB-231 cells

To test the delivery of P53 mRNA NPs in cells, the FLAG tag was labeled and observed by an immunofluorescence experiment. Briefly,

after 6 hours' incubation with P53 mRNA NPs, the cells were fixed with 4% paraformaldehyde and permeabilized with 0.4% Triton and followed by blocking with 1% bovine serum albumin (BSA) in phosphate buffered saline with Tween-20 (PBST). The FLAG tag was then labeled by anti-FLAG primary antibody (Abcam, ab-1162, 1:100 dilution) and FITC labeled secondary antibody (Abcam, ab-6717, 1:1,000 dilution). The nucleus was labeled with Hoechst 33342. The FITC and Hoechst 33342 signals were observed by a fluorescent microscope (Nikon, Japan). Stability of 4 °C stored mRNA nanoparticles was determined by measuring the size and distribution, and by detecting P53 protein using an immunofluorescence experiment at different time points.

4.7 *In vitro* cytotoxicity of chemotherapy drugs derived mRNA NPs

The cytotoxicity of different mRNA NPs was determined by MTT assay. 2,000 cells were seeded in 96 wells plate 24 h before adding different formulations. After 48 h incubation with free drug or mRNA nanoparticles, MTT was added. After another 4 h incubation, dimethyl sulfoxide (DMSO) was added to dissolve purple formazan, and the absorbance (Ab) was read at 570 nm in plate reader (MolecularDevices Spectramax M5, San Jose, CA, USA). The cell viability (%) = $(Ab_{treatment} - Ab_{blank})/ (Ab_{untreated\ control} - Ab_{blank}) \times 100\%$. The synergetic effect was calculated and analyzed by Compusyn. The absolute IC_{50} values were calculated by GraphPad Prism 6 (La Jolla, CA, USA).

4.8 *In vivo* anti-tumor efficacy studies

All animal experiments were performed in accordance with the Guidelines for Care and Use of Laboratory Animals of The Ohio State University and were approved by the Animal Ethics Committee of Institutional Animal Care and Use Committee (IACUC). 2×10^6 MDA-MB-231-luc cells in 50 μL PBS were injected in the #4 abdominal mammary gland of athymic nude female mice. Mice were randomly grouped (n = 8 in each group) when the tumor reached around 30 mm^3. Treatment with 10 mg/kg PTX or mRNA NPs (2 mg/kg mRNA) at an equivalent PTX dose was given twice a week intravenously for three weeks. Censoring of one mouse occurred in PAL ctrl mRNA NPs group on day 7 after tumor inoculation, therefore n = 7 in PAL ctrl mRNA NPs group from day 8, and n = 8 in other groups. Tumor volume was checked by digital caliper every day. Removal criteria for the tumor bearing mice were either length of tumor longer than 1.6 cm, body factor smaller than 2 or moistness or seeping in the ulceration area shown on tumor. Mice body weight was measured before each treatment during the 6 dosages. The tumor volume = length × $(width)^2/2$. PTX was first dissolved in Cremophor® EL/ethanol (50:50, v/v) and then diluted in PBS. To image P53 protein *in vivo*, tumor tissue was dissected 24 h after the last dose of PAL P53 mRNA NPs and fixed in 4% paraformaldehyde. After fixation, the tumor tissue was immersed in 30% sucrose solution overnight. The 8 μm tumor section was then prepared using the cryostat section method. Finally, the FLAG tag and nucleus were labeled and imaged using same methods mentioned above.

4.9 Statistical analysis

All statistical analyses were conducted on R3.4.3 (The R Foundation). Student's t tests were used to analyze *in vitro* data; the *in vivo* efficacy data were analyzed using two-way ANOVA with repeated measurements; the survival of tumor bearing mice was analyzed using log rank tests. All tests were two-tailed and $p < 0.05$ was considered statistically significant.

Acknowledgements

This work was supported by the Maximizing Investigators' Research Award R35GM119679 from the National Institute of General Medical Sciences as well as the start-up fund from the College of Pharmacy at The Ohio State University. C. X. Z. acknowledges the support from the Professor Sylvan G. Frank Graduate Fellowship.

Electronic Supplementary Material: Supplementary material (synthesis of PAL, optimization of PAL mRNA NPs, and *in vivo* imaging of a PAL P53 mRNA NPs treated mouse) is available in the online version of this article at https://doi.org/10.1007/s12274-019-2308-9.

References

[1] Denkert, C.; Liedtke, C.; Tutt, A.; von Minckwitz, G. Molecular alterations in triple-negative breast cancer—The road to new treatment strategies. *Lancet* **2017**, *389*, 2430–2442.

[2] The National Comprehensive Cancer Network. *NCCN Clinical Practice Guidelines in Oncology: Breast Cancer* (*Version I. 2018-March 20, 2018*) [Online]. 2018; https://www.nccn.org/professionals/physician_gls/pdf/breast.pdf (accessed Jun 1, 2018).

[3] Bianchini, G.; Balko, J. M.; Mayer, I. A.; Sanders, M. E.; Gianni, L. Triple-negative breast cancer: Challenges and opportunities of a heterogeneous disease. *Nat. Rev. Clin. Oncol.* **2016**, *13*, 674–690.

[4] Mehta, R. S.; Barlow, W. E.; Albain, K. S.; Vandenberg, T. A.; Dakhil, S. R.; Tirumali, N. R.; Lew, D. L.; Hayes, D. F.; Gralow, J. R.; Livingston, R. B. et al. Combination anastrozole and fulvestrant in metastatic breast cancer. *N. Engl. J. Med.* **2012**, *367*, 435–444.

[5] Gandhi, L.; Rodríguez-Abreu, D.; Gadgeel, S.; Esteban, E.; Felip, E.; De Angelis, F.; Domine, M.; Clingan, P.; Hochmair, M. J.; Powell, S. F. et al. Pembrolizumab plus chemotherapy in metastatic non-small-cell lung cancer. *N. Engl. J. Med.* **2018**, *378*, 2078–2092.

[6] Schmid, P.; Park, Y. H.; Muñoz-Couselo, E.; Kim, S. B.; Sohn, J.; Im, S. A.; Holgado, E.; Wang, Y.; Dang, T.; Aktan, G. et al. Pembrolizumab (pembro) + chemotherapy (chemo) as neoadjuvant treatment for triple negative breast cancer (TNBC): Preliminary results from KEYNOTE-173. *J. Clin. Oncol.* **2017**, *35*, 556–556.

[7] Wang, Y. W.; Sun S. Y.; Zhang, Z. Y.; Shi D. L. Nanomaterials for cancer precision medicine. *Adv. Mater.* **2018**, *30*, 1705660.

[8] Cancer Genome Atlas Network. Comprehensive molecular portraits of human breast tumours. *Nature* **2012**, *490*, 61–70.

[9] Morris, L. G. T.; Chan, T. A. Therapeutic targeting of tumor suppressor genes. *Cancer* **2015**, *121*, 1357–1368.

[10] Bae, Y. H.; Shin, J. M.; Park, H. J.; Jang, H. O.; Bae, M. K.; Bae, S. K. Gain-of-function mutant p53-R280K mediates survival of breast cancer cells. *Genes Genomics* **2014**, *36*, 171–178.

[11] Sahin, U.; Karikó, K.; Türeci, Ö. mRNA-based therapeutics—Developing a new class of drugs. *Nat. Rev. Drug Discov.* **2014**, *13*, 759–780.

[12] Weissman, D. mRNA transcript therapy. *Expert Rev. Vaccines* **2015**, *14*, 265–281.

[13] Yamamoto, A.; Kormann, M.; Rosenecker, J.; Rudolph, C. Current prospects for mRNA gene delivery. *Eur. J. Pharm. Biopharm.* **2009**, *71*, 484–489.

[14] Islam, M. A.; Reesor, E. K. G.; Xu, Y. J.; Zope, H. R.; Zetter, B. R.; Shi, J. J. Biomaterials for mRNA delivery. *Biomater. Sci.* **2015**, *3*, 1519–1533.

[15] Guan, S.; Rosenecker, J. Nanotechnologies in delivery of mRNA therapeutics using nonviral vector-based delivery systems. *Gene Ther.* **2017**, *24*, 133–143.

[16] Hajj, K. A.; Whitehead, K. A. Tools for translation: Non-viral materials for therapeutic mRNA delivery. *Nat. Rev. Mater.* **2017**, *2*, 17056.

[17] Li, B.; Zhang, X. F.; Dong, Y. Z. Nanoscale platforms for messenger RNA delivery. *Wiley Interdiscip. Rev. Nanomed. Nanobiotechnol.* **2018**, e1530.

[18] Liu, L. N.; Wang, Y. H.; Miao, L.; Liu, Q.; Musetti, S.; Li, J.; Huang, L. Combination immunotherapy of MUC1 mRNA nano-vaccine and CTLA-4 blockade effectively inhibits growth of triple negative breast cancer. *Mol. Ther.* **2018**, *26*, 45–55.

[19] Islam, M. A.; Xu, Y. J.; Tao, W.; Ubellacker, J. M.; Lim, M.; Aum, D.; Lee, G. Y.; Zhou, K.; Zope, H.; Yu, M. et al. Restoration of tumour-growth suppression *in vivo* via systemic nanoparticle-mediated delivery of PTEN mRNA. *Nat. Biomed. Eng.* **2018**, *2*, 850–864.

[20] Haabeth, O. A. W.; Blake, T. R.; McKinlay, C. J.; Waymouth, R. M.; Wender, P. A.; Levy, R. mRNA vaccination with charge-altering releasable transporters elicits human T cell responses and cures established tumors in mice. *Proc. Natl. Acad. Sci. USA* **2018**, *115*, E9153–E9161.

[21] Van Hoecke, L.; Van Lint, S.; Roose, K.; Van Parys, A.; Vandenabeele, P.; Grooten, J.; Tavernier, J.; De Koker, S.; Saelens, X. Treatment with mRNA coding for the necroptosis mediator MLKL induces antitumor immunity directed against neo-epitopes. *Nat. Commun.* **2018**, *9*, 3417.

[22] Kranz, L. M.; Diken, M.; Haas, H.; Kreiter, S.; Loquai, C.; Reuter, K. C.; Meng, M.; Fritz, D.; Vascotto, F.; Hefesha, H. et al. Systemic RNA delivery to dendritic cells exploits antiviral defence for cancer immunotherapy. *Nature* **2016**, *534*, 396–401.

[23] Oberli, M. A.; Reichmuth, A. M.; Dorkin, J. R.; Mitchell, M. J.; Fenton, O. S.; Jaklenec, A.; Anderson, D. G.; Langer, R.; Blankschtein, D. Lipid nanoparticle assisted mRNA delivery for potent cancer immunotherapy. *Nano Lett.* **2017**, *17*, 1326–1335.

[24] Cheng, Q.; Wei, T.; Jia, Y. M.; Farbiak, L.; Zhou, K. J.; Zhang, S. Y.; Wei, Y. L.; Zhu, H.; Siegwart, D. J. Dendrimer-based lipid nanoparticles deliver therapeutic FAH mRNA to normalize liver function and extend survival in a mouse model of hepatorenal tyrosinemia type I. *Adv. Mater.* **2018**, *30*, 1805308.

[25] Miller, J. B.; Zhang, S. Y.; Kos, P.; Xiong, H.; Zhou, K. J.; Perelman, S. S.; Zhu, H.; Siegwart, D. J. Non-Viral CRISPR/Cas gene editing *in vitro* and *in vivo* enabled by synthetic nanoparticle co-delivery of Cas9 mRNA and sgRNA. *Angew. Chem., Int. Ed.* **2017**, *56*, 1059–1063.

[26] Robinson, E.; MacDonald, K. D.; Slaughter, K.; McKinney, M.; Patel, S.; Sun, C.; Sahay, G. Lipid nanoparticle-delivered chemically modified mRNA Restores chloride secretion in cystic fibrosis. *Mol. Ther.* **2018**, *26*, 2034–2046.

[27] Gurnani, M.; Lipari, P.; Dell, J.; Shi, B.; Nielsen, L. L. Adenovirus-mediated p53 gene therapy has greater efficacy when combined with chemotherapy against human head and neck, ovarian, prostate, and breast cancer. *Cancer Chemother. Pharmacol.* **1999**, *44*, 143–151.

[28] Jiang, C.; Mei, M.; Li, B.; Zhu, X. R.; Zu, W. H.; Tian, Y. J.; Wang, Q. N.; Guo, Y.; Dong, Y. Z.; Tan, X. A non-viral CRISPR/Cas9 delivery system for therapeutically targeting HBV DNA and *pcsk9 in vivo*. *Cell Res.* **2017**, *27*, 440–443.

[29] Jia, L. Nanoparticle formulation increases oral bioavailability of poorly soluble drugs: Approaches, experimental evidences and theory. *Curr. Nanosci.* **2005**, *1*, 237–243.

[30] Doane, T.; Burda, C. Nanoparticle mediated non-covalent drug delivery. *Adv. Drug Deliv. Rev.* **2013**, *65*, 607–621.

[31] Sofias, A. M.; Dunne, M.; Storm, G.; Allen, C. The battle of "nano" paclitaxel. *Adv. Drug Deliv. Rev.* **2017**, *122*, 20–30.

[32] Ye, L.; He, J.; Hu, Z. P.; Dong, Q. J.; Wang, H. B.; Fu, F. H.; Tian, J. W. Antitumor effect and toxicity of Lipusu in rat ovarian cancer xenografts. *Food Chem. Toxicol.* **2013**, *52*, 200–206.

[33] Oudin, M. J.; Barbier, L.; Schäfer, C.; Kosciuk, T.; Miller, M. A.; Han, S.; Jonas, O.; Lauffenburger, D. A.; Gertler, F. B. MENA confers resistance to paclitaxel in triple-negative breast cancer. *Mol. Cancer Ther.* **2017**, *16*, 143–155.

[34] Conley, S. J.; Baker, T. L.; Burnett, J. P.; Theisen, R. L.; Lazarus, D.; Peters, C. G.; Clouthier, S. G.; Eliasof, S.; Wicha, M. S. CRLX101, an investigational camptothecin-containing nanoparticle-drug conjugate, targets cancer stem cells and impedes resistance to antiangiogenic therapy in mouse models of breast cancer. *Breast Cancer Res. Treat.* **2015**, *150*, 559–567.

[35] Li, B.; Luo, X.; Deng, B. B.; Wang, J. F.; McComb, D. W.; Shi, Y. M.; Gaensler, K. M. L.; Tan, X.; Dunn, A. L.; Kerlin, B. A. et al. An Orthogonal array optimization of lipid-like nanoparticles for mRNA delivery *in vivo*. *Nano Lett.* **2015**, *15*, 8099–8107.

[36] Zhang, X. F.; Li, B.; Luo, X.; Zhao, W. Y.; Jiang, J.; Zhang, C. X.; Gao, M.; Chen, X. F.; Dong, Y. Z. Biodegradable amino-ester nanomaterials for Cas9 mRNA delivery *in vitro* and *in vivo*. *ACS Appl. Mater. Interfaces* **2017**, *9*, 25481–25487.

[37] Li, B.; Luo, X.; Deng, B. B.; Giancola, J. B.; McComb, D. W.; Schmittgen, T. D.; Dong, Y. Z. Effects of local structural transformation of lipid-like compounds on delivery of messenger RNA. *Sci. Rep.* **2016**, *6*, 22137.

[38] Muller, P. A. J.; Vousden, K. H. Mutant p53 in cancer: New functions and therapeutic opportunities. *Cancer Cell* **2014**, *25*, 304–317.

[39] Weiss, R. B.; Donehower, R. C.; Wiernik, P. H.; Ohnuma, T.; Gralla, R. J.; Trump, D. L.; Baker, J. R. B. Jr.; Van Echo, D. A.; Von Hoff, D. D.; Leyland-Jones, B. Hypersensitivity reactions from taxol. *J. Clin. Oncol.* **1990**, *8*, 1263–1268.

[40] Balaji, B. S.; Lewis, M. R. Double exponential growth of aliphatic polyamide dendrimers via AB_2 hypermonomer strategy. *Chem. Commun.* (*Camb.*) **2009**, 4593–4595.

[41] Gjoerup, O.; Zaveri, D.; Roberts, T. M. Induction of p53-independent apoptosis by simian virus 40 small t antigen. *J. Virol.* **2001**, *75*, 9142–9155.

[42] Kauffman, K. J.; Dorkin, J. R.; Yang, J. H.; Heartlein, M. W.; DeRosa, F.; Mir, F. F.; Fenton, O. S.; Anderson, D. G. Optimization of lipid nanoparticle formulations for mRNA Delivery *in vivo* with fractional factorial and definitive screening designs. *Nano Lett.* **2015**, *15*, 7300–7306.